

# Spin Correlations and Magnetic Order in Nonsuperconducting $\text{Nd}_{2-x}\text{Ce}_x\text{CuO}_{4\pm\delta}$

P.K. Mang<sup>1</sup>, O.P. Vajk<sup>2</sup>, A. Arvanitaki<sup>2</sup>, J.W. Lynn<sup>3</sup>, and M. Greven<sup>1,4</sup>

<sup>1</sup>*Department of Applied Physics, Stanford University, Stanford, CA 94305*

<sup>2</sup>*Department of Physics, Stanford University, Stanford, CA 94305*

<sup>3</sup>*NIST Center for Neutron Research, National Institute for Standards and Technology, Gaithersburg, Maryland 20899 and*

<sup>4</sup>*Stanford Synchrotron Radiation Laboratory, Stanford, CA 94309*

(Dated: January 29, 2020)

We report quantitative neutron scattering measurements of the evolution with doping of the Néel temperature, the antiferromagnetic correlations, and the ordered moment of as-grown, non-superconducting  $\text{Nd}_{2-x}\text{Ce}_x\text{CuO}_{4\pm\delta}$  ( $0 \leq x \leq 0.18$ ). The instantaneous correlation length can be effectively described by our quantum Monte Carlo calculations for the randomly site-diluted nearest-neighbor spin-1/2 square-lattice Heisenberg antiferromagnet. However, quantum fluctuations have a stronger effect on the ordered moment, which decreases more rapidly than for the quenched-disorder model.

PACS numbers: 74.25.Ha, 75.40.Mg, 75.50.Ee

Over the past eighteen years much has been learned about the evolution with doping of magnetic correlations in the high-temperature superconductors. For the prototypical material  $\text{La}_{2-x}\text{Sr}_x\text{CuO}_4$  (LSCO), neutron scattering has led to the observation of the loss of long-range antiferromagnetic order and the concomitant decrease of two-dimensional (2D) spin correlations [1], an incommensurate spin-density wave [2], and coupled charge and magnetic “stripe” order upon co-doping with Nd [3]. The richness of the observed behavior is attributable to the evolution of the cuprate superconductors from Mott-insulating parent materials which are found to be excellent realizations, at low energies and long wavelengths, of the spin-1/2 square-lattice Heisenberg antiferromagnet (SLHAF) [4]. Although the vast majority of research has focused on the hole-doped systems, the electron-doped materials, typified by  $\text{Nd}_{2-x}\text{Ce}_x\text{CuO}_{4\pm\delta}$  (NCCO) [5], have presented an important challenge to the field of high- $T_c$  research and particularly to the paradigm established from experiments on LSCO. Unlike for LSCO, the magnetic phase of NCCO is very robust with respect to doping [6, 7, 8] and the magnetic correlations remain commensurate [8, 9].

Since superconductivity in the high- $T_c$  cuprates appears in close proximity to antiferromagnetic phases, it is essential to understand the nature of nearby magnetic ground states. As-grown, NCCO is not superconducting, and the antiferromagnetic phase extends to the highest concentration for which samples can be produced ( $x \approx 0.18$ ). Oxygen impurities are believed to occupy the nominally vacant apical sites [10], and a relatively severe oxygen reduction procedure must be applied to induce superconductivity above  $x = 0.13$  [5]. Although the reduction procedure weakens the magnetism, magnetic order is still observed near optimal doping where  $T_c = 24$  K [8, 11]. One qualitative argument often employed to explain the robustness of the antiferromagnetic phase in the electron-doped cuprates is that, whereas hole carriers are doped into the O 2p band and frustrate the antiferro-

magnetic arrangement of the neighboring Cu ions, doped electrons primarily reside on the Cu site, filling the 3d shell and removing the spin degree of freedom [6, 7, 8]. New, quantitative insights have been gained recently into the role of *static* non-magnetic impurities introduced into the spin-1/2 SLHAF [12, 13, 14, 15], and it would be interesting to test how well NCCO can be described by this model.

In this Letter, we present detailed neutron scattering results on the evolution with Ce doping of the magnetic properties of as-grown, non-superconducting  $\text{Nd}_{2-x}\text{Ce}_x\text{CuO}_{4\pm\delta}$  ( $0 \leq x \leq 0.18$ ). We find that the instantaneous spin correlations in the paramagnetic phase are, in effect, well described by the randomly-diluted spin-1/2 nearest-neighbor (NN) SLHAF model for which we have carried out numerical simulations. On the other hand, the ordered moment falls off more rapidly, a clear indication that quantum fluctuations are stronger than for the model magnet and that such fluctuations manifest themselves differently for different observables. We also find that the primary difference between the Néel temperature and ordered moment of as-grown and reduced NCCO is a shift in electron concentration that corresponds to  $|\Delta x| \approx 0.03$ .

Crystals of  $\text{Nd}_{2-x}\text{Ce}_x\text{CuO}_{4\pm\delta}$  were grown in 4 atm of  $\text{O}_2$  using the traveling-solvent floating-zone technique. The solubility limit is about  $x = 0.18$ , and our study spans the range  $0 \leq x \leq 0.18$ . In addition, several samples were reduced for 20 h at 960°C in Ar followed by an anneal for 20 h at 500°C in  $\text{O}_2$  for additional magnetic order parameter measurements. Magnetometry indicates that the reduced  $x = 0.14$  and  $x = 0.18$  samples are superconducting with  $T_c = 24$  K and 20 K (onset), respectively. Our single-grain crystals are cylindrical, typically with a diameter of 4.5 mm, and range in volume from 0.1 to 0.7  $\text{cm}^3$ . Average Ce concentrations were verified using inductively coupled plasma spectroscopy and typically found to equal the nominal values. The neutron scattering measurements were performed on the thermal

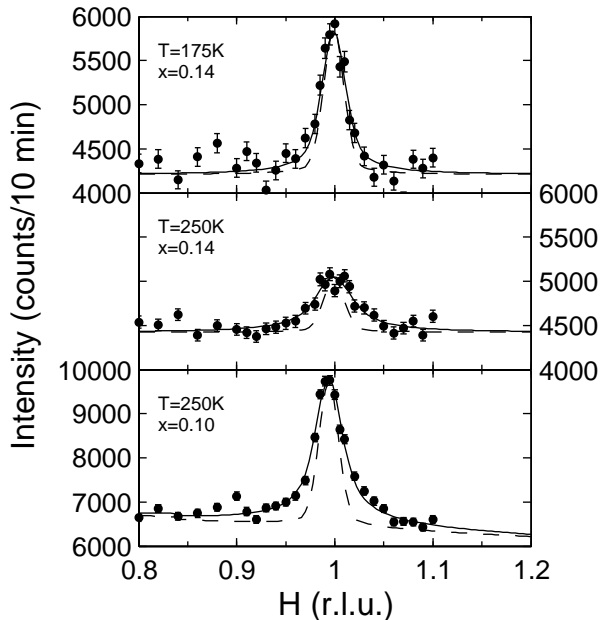


FIG. 1: Representative two-axis scans for  $x = 0.10$  and  $0.14$  along  $\mathbf{q}_{2D} = (H/2 - 1/2, H/2 - 1/2)$  in the paramagnetic phase with collimations  $40^\circ$ - $42.5^\circ$ -sample- $23.7^\circ$  and incident neutron energy  $E_i = 14.7$  meV. The instrumental resolution is indicated by the dashed lines.

triple-axis instruments BT2 and BT9 of the NIST Center for Neutron Research.

All as-grown samples exhibit long-range magnetic order at low temperature. However, significant two-dimensional (2D) magnetic correlations are already present well above the Néel temperature [8]. These may be probed through “two-axis” scans in which one integrates the dynamic structure factor  $S(\mathbf{q}_{2D}, \omega)$  over the limits set by the thermal energy,  $-k_B T$ , and the incident neutron energy,  $E_i$ . If the integration is carried out over the relevant fluctuations one obtains the equal-time structure factor  $S(\mathbf{q}_{2D})$  [4]. In Fig. 1, we present representative scans of this type that show a peak in  $S(\mathbf{q}_{2D})$  at the incipient antiferromagnetic ordering wavevector. We fit these data to a 2D Lorentzian,  $S(q_{2D}) = S(0)/(1 + q_{2D}^2 \xi^2)$ , convolved with the instrumental resolution. As the temperature or the doping level is increased, correlations decrease, which manifests itself as a broadening of the observed peaks.

Figure 2 summarizes the behavior of  $\xi(x, T)$  for several Ce concentrations. Over a wide temperature range, the spin correlations exhibit an exponential dependence on inverse temperature,  $\xi(x, T) \sim \exp(2\pi\rho_s(x)/T)$  with spin stiffness  $\rho_s(x)$ , indicative of an underlying ground state with 2D antiferromagnetic order [16]. We overlay the results of quantum Monte Carlo simulations for the randomly-diluted SLHAF, described by the Hamiltonian

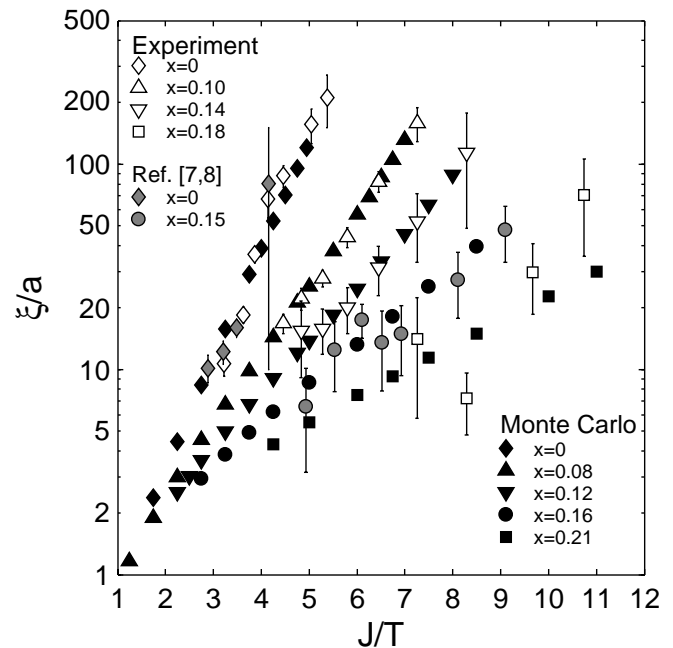


FIG. 2: Semi-log plot of the magnetic correlation length (in units of the lattice constant  $a$ ) versus inverse temperature (in units of  $J = 125$  meV  $\approx 1450$  K) for  $x = 0, 0.10, 0.14$ , and  $0.18$ . The data terminate just above the onset of Néel order at low temperature. Also displayed are previous data for  $x = 0$  and  $x = 0.15$  [7, 8] and Quantum Monte Carlo results for Eq. (1).

$$\mathcal{H} = J \sum_{\langle i, j \rangle} p_i p_j \mathbf{S}_i \cdot \mathbf{S}_j, \quad (1)$$

where the sum is over NN sites,  $J$  is the antiferromagnetic Cu-O-Cu superexchange,  $\mathbf{S}_i$  is the spin-1/2 operator at site  $i$ ,  $p_i = 1$  on magnetic sites, and  $p_i = 0$  on nonmagnetic sites. The numerical method is the same as that employed previously [14]. The data are plotted as  $\xi/a$ , the ratio of the spin-spin correlation length to the NN Cu-Cu distance ( $a \approx 3.95$  Å), versus  $J/T$ , the ratio of the NN antiferromagnetic superexchange of  $\text{Nd}_2\text{CuO}_4$  to the temperature. A previous estimate from comparison of  $\xi(T)$  with theory for the SLHAF yielded  $J \approx 130$  meV [7], and we find  $J = 125(4)$  meV from comparison with our numerical results for  $x = 0$ . Since the value of  $J$  has been established, the only adjustable parameter in the comparison for the Ce-doped samples is the concentration of non-magnetic sites in Eq. (1). We find good qualitative agreement among experiment and Monte Carlo if we fix this concentration to equal the nominal Ce concentration  $x$ . However, as shown in Fig. 2, the agreement becomes quantitative if we allow the effective dilution to differ slightly:  $x_{\text{eff}}(x = 0.10) = 0.08(1)$ ,  $x_{\text{eff}}(x = 0.14) = 0.12(1)$ , and  $x_{\text{eff}}(x = 0.18) = 0.21(2)$ . Also shown are previous data for as-grown samples with  $x = 0$  and  $x = 0.15$  [7, 8]. The

result for  $\text{Nd}_2\text{CuO}_4$  agrees well with ours, and we estimate that  $x_{\text{eff}}(x = 0.15) = 0.16(2)$ . The extent to which the quenched-disorder model Eq. (1) effectively describes the spin correlations of as-grown, non-superconducting NCCO is remarkable. The observed small differences between nominal electron concentration and effective static dilution may be in part due to the uncertainty in the oxygen (and hence electron) concentration of our samples. Another likely possibility is the presence of additional quantum fluctuations which are not captured in the effective Hamiltonian Eq. (1), for example due to frustrating next-NN interactions.

The spin stiffness of the disorder-free spin-1/2 NN SLHAF is known to be  $2\pi\rho_s/J = 1.131(3)$  [17]. An estimate for the case of quenched disorder, Eq. (1), has been obtained in previous numerical work [14]. Comparison of the experimental results in Fig. 2 gives the effective values  $2\pi\rho_s/J = 0.71(2)$ ,  $0.54(4)$ ,  $0.40(7)$ , and  $0.25(5)$ , respectively, for  $x = 0.10$ ,  $0.14$ ,  $0.15$ , and  $0.18$ . The value  $0.40(7)$  for the  $x = 0.15$  sample is somewhat smaller than the original estimate of  $2\pi\rho_s/J \approx 0.54$  [8] which was based on a classical rather than a quantum [14] picture for the doping dependence of the spin stiffness.

We note that Ref. [8] reports data for two as-grown  $x = 0.15$  samples with onset of magnetic order at  $T_N = 160$  and  $125$  K. If we allow for a distribution of Néel temperatures to account for the rounding of the observed transition, we estimate mean values of  $T_N = 147(17)$  and  $115(9)$  K, respectively. This is consistent with how we have treated our own data. The second sample from Ref. [8] also exhibits lower values of  $\xi(T)$  (not shown in Fig. 2), comparable to our  $x = 0.18$  crystal. The removal of oxygens through the reduction process changes both the degree of disorder and the carrier concentration. This lowers the Néel temperature and, for  $x > 0.13$ , leads to a decrease of the antiferromagnetic volume fraction and to bulk superconductivity [11]. Growth at lower oxygen partial pressure mimics the reduction process, resulting in lower oxygen contents and higher effective doping levels. The primary focus of this Letter is on non-superconducting, as-grown NCCO, and therefore we were careful to grow our samples under high oxygen partial pressure, resulting in crystals with  $T_N$  at or close to the maximum value attainable.

Figure 3(a) indicates that the Néel temperature  $T_N(x)$  of our as-grown samples, as obtained from neutron diffraction, approximately follows a parabolic form, extrapolating to zero at  $x \approx 0.21$ . As shown in Fig. 3(a), qualitatively similar behavior has previously been found for reduced NCCO for which  $T_N(x)$  is lower [18]. The primary effect of the reduction is an approximately rigid shift by  $|\Delta x| \approx 0.03$  due to the change in carrier density. The concave doping dependence for NCCO is contrasted by the behavior exhibited by the randomly-diluted spin-1/2 SLHAF  $\text{La}_2\text{Cu}_{1-x}(\text{Zn,Mg})_x\text{O}_4$  (LCZMO), for which Néel order extends up to the site percolation threshold,

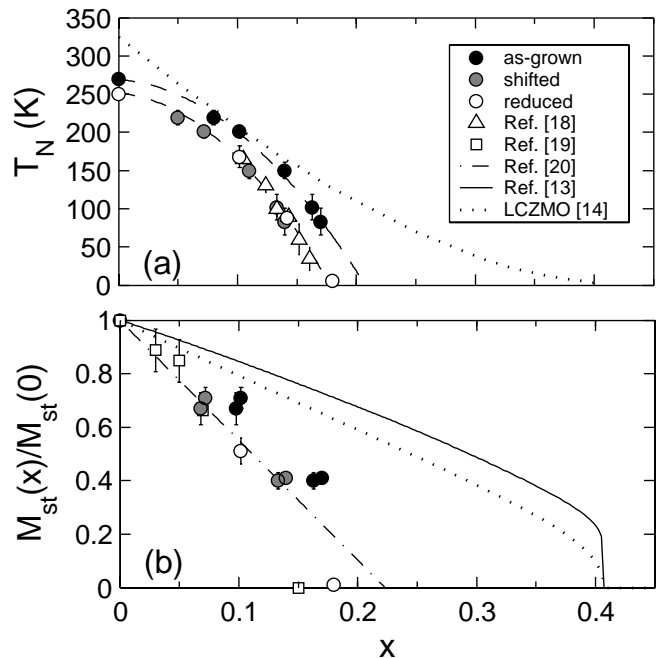


FIG. 3: (a) Néel temperature doping dependence. Ce-doped samples exhibit some rounding in the transition due to oxygen and cerium inhomogeneities, which is represented by the error bars. Results for a previous study [18] of reduced samples are shown for comparison (triangles). The dashed curves are quadratic fits, and the dotted line indicates the behavior observed for LCZMO [14]. The grey circles are the as-grown data shifted by  $|\Delta x| = 0.03$ . (b) Doping dependence of the ordered copper moment per site, normalized by the value for  $\text{Nd}_2\text{CuO}_4$ . The grey circles are the as-grown data shifted by  $|\Delta x| = 0.03$ . The squares are data obtained in a previous study [19] and the dot-dashed line is a recent theoretical prediction [20]. For comparison, Monte Carlo results for the diluted SLHAF (solid line) [13] and the behavior observed for LCZMO (dotted line) [14] are indicated as well.

$x_p \approx 0.41$ , and the 2D spin correlations are quantitatively described by Eq. (1) up to  $x_p$  [14].

In Fig. 3(b), we plot the ordered moment for several samples, as obtained from order parameter measurements at low temperature. The values are normalized to that of  $\text{Nd}_2\text{CuO}_4$ . Consistent with the behavior of  $T_N(x)$ , the moment of as-grown NCCO approaches zero much more rapidly than in the case of random dilution: at the rate  $1 - M_{\text{st}}(x)/M_{\text{st}}(0) \approx 3.5x$  which is approximately twice that of the diluted spin-1/2 SLHAF for  $x < 0.20$ . On the other hand, the magnetic phase extends much further than for LSCO [1] and Li-doped  $\text{La}_2\text{CuO}_4$  [21], for which Néel order is destroyed above  $x \approx 0.02$  and  $x \approx 0.03$ , respectively. The moment of reduced samples is lowered further. We note that these data are again normalized by the value for as-grown  $\text{Nd}_2\text{CuO}_4$ , and that a rigid shift of  $|\Delta x| = 0.03$  leads to a good agreement of the two data sets. Our result is consistent with previous experimental work at lower concentrations [19].

If viewed instantaneously, so as to mitigate the effects due to the increased itinerancy upon doping, the magnetism of NCCO should indeed resemble a system with quenched random site dilution. What is surprising is that for  $\xi(x, T)$  the correspondence with Eq. (1) is nearly quantitative. Since the charge carriers in as-grown NCCO are itinerant, even well below  $T_N$  [22], deviations from the static model Eq. (1) may be expected to emerge as we view the two systems on different time scales. Indeed, the ordered moment, a measure of the strength of the magnetic order at infinitely long times, decreases much more rapidly in the case of NCCO than for the SLHAF. We note that slight deviations, possibly due to the presence of a frustrating next-NN exchange, are already observable for the ordered moment of LCZMO [14] (Fig. 3(b)), and that LCZMO appears to be in close proximity to a new quantum critical point in an extended parameter space [15]. In the case of LCZMO, these perturbations are not quite strong enough to shift the critical point away from the geometric site-percolation threshold. Although the experimentally accessible doping range is limited, our results for NCCO are consistent with the existence of a quantum critical point below the geometric site-percolation threshold.

We note that recent calculations for the one-band Hubbard model are in semi-quantitative agreement with our data for the spin correlations [20, 23] and ordered moment [20, 24, 25]. The latter result is shown in Fig. 3(b). These theories were motivated by photoemission measurements of the evolution of the Fermi surface of reduced  $\text{Nd}_{2-x}\text{Ce}_x\text{CuO}_{4\pm\delta}$  ( $0 \leq x \leq 0.15$ ) [26]. Their proponents assert that  $t - J$  models are intrinsically limited in describing the electron-doped cuprates and that a proper description requires  $t - U$  models with a decreasing value of  $U$  with increasing electron concentration [20, 23, 24, 27].

In summary, we have presented a comprehensive neutron scattering study of the magnetic properties of non-superconducting  $\text{Nd}_{2-x}\text{Ce}_x\text{CuO}_{4\pm\delta}$ . Although the evolution of the instantaneous spin-correlations may effectively be described by a site-dilution model, a proper description of the magnetic degrees of freedom must necessarily include the effects of electron itinerancy. While the achievements of recent theoretical treatments of the Hubbard model seem very promising, it is not clear at present if this model exhibits a superconducting ground state. Phonon anomalies have been observed in both electron and hole doped high-temperature superconductors [28], and a complete description of these materials may require the additional consideration of the electron-lattice coupling. Regardless, our data should serve as a benchmark for tests of still-emerging theories for the high- $T_c$  phase diagram.

We acknowledge valuable discussions with N.P. Armitage, S. Larochelle, R.S. Markiewicz, M. Matsuda,

and A.-M. S. Tremblay, and thank I. Tanaka and the late H. Kojima for their invaluable assistance during the initial stage of the crystal growth effort. This work was supported by the US Department of Energy under Contracts No. DE-FG03-99ER45773 and No. DE-AC03-76SF00515, and by NSF CAREER Award No. DMR9985067.

- 
- [1] B. Keimer *et al.*, Phys. Rev. B **46**, 14034 (1992), and references therein.
  - [2] K. Yamada *et al.*, Phys. Rev. B **57**, 6165 (1998), and references therein.
  - [3] J. M. Tranquada *et al.*, Nature (London) **375**, 561 (1995).
  - [4] R. J. Birgeneau *et al.*, Phys. Rev. B **59**, 13788 (1999).
  - [5] Y. Tokura, H. Takagi, and S. Uchida, Nature **337**, 345 (1989).
  - [6] G.M. Luke *et al.*, Phys. Rev. B **42**, 7981 (1990).
  - [7] T. R. Thurston *et al.*, Phys. Rev. Lett. **65**, 263 (1990).
  - [8] M. Matsuda *et al.*, Phys. Rev. B **45**, 12548 (1992).
  - [9] K. Yamada, K. Kurahashi, Y. Endoh, R. J. Birgeneau, and G. Shirane, J. Phys. Chem. Solids **60**, 1025 (1999).
  - [10] A. J. Schultz, J. D. Jorgensen, J. L. Peng, and R. L. Greene, Phys. Rev. B **53**, 5157 (1996).
  - [11] T. Uefuji *et al.*, Physica C **357-360**, 273 (2001).
  - [12] S. Sachdev, C. Buragohain, and M. Vojta, Science **286**, 2479 (1999).
  - [13] A. W. Sandvik, Phys. Rev. B **66**, 024418 (2002).
  - [14] O. P. Vajk *et al.*, Science **295**, 1691 (2002); O. P. Vajk, M. Greven, P. K. Mang, and J. W. Lynn, Solid State Comm. **126**, 93 (2003).
  - [15] A. W. Sandvik, Phys. Rev. Lett. **89**, 177201 (2002); O. P. Vajk and M. Greven, Phys. Rev. Lett. **89**, 172202 (2002).
  - [16] S. Chakravarty, B. I. Halperin, and D. R. Nelson, Phys. Rev. B **39**, 2344 (1989).
  - [17] B. B. Beard, R. J. Birgeneau, M. Greven, and U.-J. Wiese, Phys. Rev. Lett. **80**, 1742 (1998).
  - [18] T. Uefuji *et al.*, Physica C **378-381**, 273 (2002).
  - [19] M. Rosseinsky, K. Prassides, and P. Day, Inorg. Chem. **30**, 2680 (1991).
  - [20] R. S. Markiewicz, cond-mat/0312594.
  - [21] T. Sasagawa *et al.*, Phys. Rev. B **66**, 184512 (2002).
  - [22] The planar resistivity at 4.2 K is as low as  $\rho \sim 2 \text{ m}\Omega \text{ cm}$  for as-grown NCCO ( $x = 0.15$ ): Y. Onose *et al.*, Phys. Rev. Lett. **82**, 5120 (1999).
  - [23] B. Kyung, V. Hankevych, A.-M. Daré, and A.-M. S. Tremblay, cond-mat/0312499.
  - [24] C. Kusko, R.S. Markiewicz, M. Lindroos and A. Bansil, Phys. Rev. B **66**, 140513 (2002).
  - [25] Ref. [24] is a mean-field theory. Up to  $x = 0.10$ , quantum fluctuations were found to lower  $M_{\text{st}}(x)$  by  $1/\eta \sim 0.78 - 0.84$ , so the ratio  $M_{\text{st}}(x)/M_{\text{st}}(0)$  remains approximately unaltered; the linear behavior at higher concentrations is to be viewed as an upper bound [20].
  - [26] N. P. Armitage *et al.*, Phys. Rev. Lett. **88**, 257001 (2002).
  - [27] D. Sénéchal and A.-M.S. Tremblay, Phys. Rev. Lett. **92**, 126401 (2004).
  - [28] M. d'Astuto *et al.*, Phys. Rev. Lett. **88**, 167002 (2002), and references therein.